Supporting Information

pH-controlled self-assembled fibrillar network (SAFiN) hydrogels: evidence of a kinetic control of the mechanical properties

Ghazi Ben Messaoud,[a,†] Patrick Le Griel,[a] Daniel Hermida-Merino,[b] Sophie L. K. W. Roelants,[c,d] Wim Soetaert,[c] Christian Victor Stevens,[e] Niki Baccile[a,*]

[a] Sorbonne Université, Centre National de la Recherche Scientifique, Laboratoire de Chimie de la Matière Condensée de Paris, LCMCP, F-75005 Paris, France

[†] Current address: DWI- Leibniz Institute for Interactive Materials, Forckenbeckstrasse 50, 52056 Aachen, Germany

[b] Netherlands Organisation for Scientific Research (NWO), DUBBLE@ESRF BP CS40220, 38043 Grenoble, France

[c] Ghent University, Centre for Industrial Biotechnology and Biocatalysis (InBio.be), Coupure Links 653, Ghent, Oost-Vlaanderen, BE 9000

[d] Bio Base Europe Pilot Plant, Rodenhuizekaai 1, Ghent, Oost-Vlaanderen, BE 9000

[e] SynBioC, Department of Green Chemistry and Technology, Ghent University, Coupure Links 653, 9000 Ghent, Belgium.

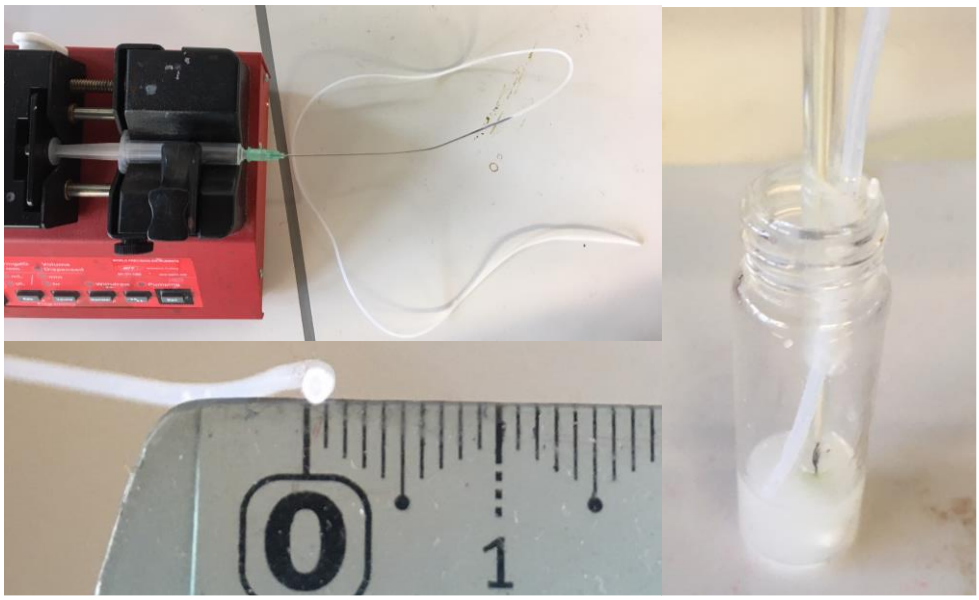

Figure S 1 – Typical push-syringe apparatus used to acidify the SLC18:0 solution (1 mL, in the image). The syringe is connected to a thin wall microbore PTFE tube, which is immerged in the solution. A pH microelectrode monitors the pH at all time during acid injection.

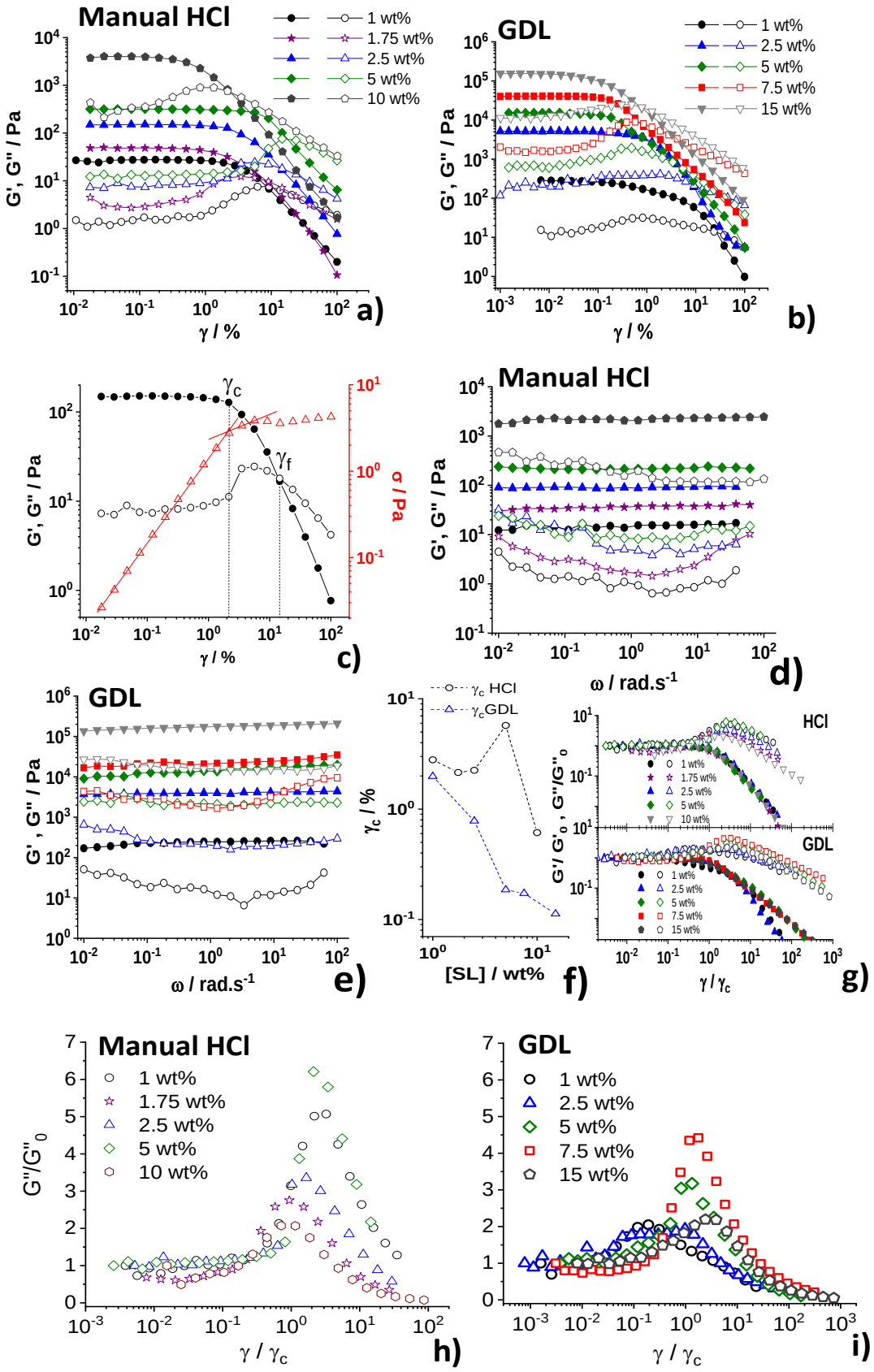

Figure S 2 - Rheological properties of SLC18:0 hydrogels at pH~6 prepared either by manual acidification using HCl or upon GDL addition (molar ratio of SLC18:0:0.63 GDL) to basic solutions (initial pH 11).

Concentration effects on the strain dependent storage (G') and loss (G'') moduli at a constant angular frequency (ω= 6.28 rad.s^{-1}) upon a) manual HCl acidification and b) GDL addition. c) Typical strain sweep curve of SLC18:0 (C= 2.5 wt%) showing how γ_c and γ_f are determined. Concentration effect on the angular frequency, ω, dependence of G' and G'' for hydrogels prepared using d) HCl or e) GDL. The legend for panel a) apply to d) and the legend for panel b) apply to e). f) Concentration effect on the critical shear strain (γ_c). g) Evolution of the reduced elastic (G'/G'_0) and viscous (G''/G''_0) reduced moduli as function of the reduced shear strain (γ/γ_c). h-i) magnification of the viscous (G''/G''_0) reduced moduli as function of the reduced shear strain (γ/γ_c) for SLC18:0 samples obtained upon h) manual HCl acidification or i) GDL addition.

The rheological properties of SLC18:0 hydrogels prepared by manual acidification using HCl or upon addition of GDL (molar ratio of SLC18:0:0.63 GDL) are shown in Figure S 2. As discussed in the main text, the shear strain dependency of storage (G') and loss (G'') moduli demonstrate the same typical behavior (Figure S 2a, b). As shear strain increases, G' decreases from a critical shear strain, γ_c (i.e, deviation from linearity), while G'' increases. The estimation of the critical shear strain γ_c is obtained from the extent of the linear relationship between the stress (σ) and the strain (γ) and where $\sigma = G^* \gamma$, with G^* being the complex modulus calculated as $G^* = (G'^2 + G''^2)^{1/2}$ (Figure S 2c). The extent of the linear viscoelastic regime from γ_c is related to structural changes and gel disruption. Finally, G' decreases gradually with increasing shear strain amplitude while G'' exhibits a small strain hardening until $G'= G''$, denoted as the fluidization strain (γ_f) from which both moduli decrease with strain, but where $G''> G'$ indicates a fluid-like behavior.

The evolution of $G'(\omega)$ and $G''(\omega)$ as function of angular frequency (ω) show that comparable concentrations (1, 2.5 and 5 wt %), $G'(\gamma)$ of hydrogels prepared using GDL are at least one order of magnitude higher than samples prepared using HCl, demonstrating the influence of the acidification method on the final stiffness of the sample (Figure S 2d,e).

The evolution of the critical shear strain γ_c as a function of concentration and acidification method (HCl or GDL) is shown in Figure S 2f. For hydrogels prepared using HCl, the critical shear strain γ_c remains practically constant with concentration for $C_{SLC18:0} \leq 5$ wt% before falling for $C_{SLC18:0}$ = 10 wt%. On the contrary, γ_c decreases significantly with concentration for the samples prepared using GDL, demonstrating that the sample becomes more brittle with increasing concentration. This phenomenon indicates that if the sample becomes stiffer due to the increase of G' with concentration, it is also more sensitive to deformation. Such decrease of γ_c with concentration has been previously observed for other

SAFiNs systems[1–3] and it is in good agreement with the theoretical prediction for sterically entangled solutions of biopolymers or cross-linked gels.[4] It is in fact known that the decrease of the theoretical γ_c with increasing concentration is attributed to the reduction of the mesh size (the average spacing between fibers) and reduction of the entanglement length (distance between entanglement points).[4]

To investigate the yielding behavior of SLC18:0 samples under large amplitude oscillatory shear (LAOS), G' and G'' moduli have been normalized by their respective values in the LVER (G'/G'_0; G''/G''_0) and plotted as a function of the reduced shear strain amplitude (γ/γ_c) (Figure S 2g). The reduced data show the decrease of G'/G'_0 and a local maximum in G''/G''_0 curves. Based on the descriptive classification of the viscoelastic properties of complex fluids as function of their LAOS behavior, SLC18:0 samples are considered as weak strain overshoot fluids.[5] All G'/G'_0 for HCl samples can be plotted on a master curve, while a small deviation at high γ/γ_c is observed for samples prepared using GDL. Such strain hardening overshoot was previously reported for a wide range of complex fluids like concentrated emulsions,[6] microgels suspensions,[7] hydrophilic[8] and hydrophobically-modified[9] polymers but also for SAFIN without discussing its origin.[10] Depending on the complex fluid, the origin of the strain overshoot can be attributed to an increase of the effective volume of temporal structures,[11] to a variation of aggregate size in suspensions[12] or to a rearrangement of clusters[13] during oscillatory shear deformation.[5] However it's generally assumed that weak strain overshoot is a result from the balance between the formation and the destruction of the network junctions.[5] In this work (refer to main text), we make the hypothesis, by combining rheology and microscopy (optical and cryo-TEM), the overshoot can be explained by the presence of spherulites and branched structures.

Figure S 2h and Figure S 2i bring out the intensity of the peak of the reduced viscous modulus (G''/G''_0) as function of the reduced shear strain (γ/γ_c) for SLC18:0 samples obtained upon manual HCl acidification or GDL addition. The intensity of the strain hardening of the reduced loss modulus (G''/G''_0) varies in a considerable manner, however it does not show a clear dependence on the SLC18:0 concentration. The global peak intensity of (G''/G''_0) was relatively higher for samples prepared by manual acidification using HCl. One could suppose that the higher presence of spherulites with an intermediate size in HCl samples compared to GDL samples, may be responsible of the strain overshoot by analogy to flocks or clusters formation in other weak strain overshoot fluids (emulsions and suspension). However the presence also of weak strain overshoot for SLC180 samples prepared upon GDL addition may

contradicts this assumption. It's worth mentioning that hydrophilic polymers like xanthan gum showed also a weak strain overshoot related to the formation of intermediate structural complex by the association of the extended chains by hydrogen bonding.[8] The formation of intermediate structural complex between SLC18:0 ribbons by inter-ribbons interactions should not be excluded. Under large deformations, these complex structures will first resist against the imposed deformation resulting in an increase in G'', before they break up from a certain deformation limit beyond which the SLC180 fibers align with the flow field and resulting in a decrease in G''.

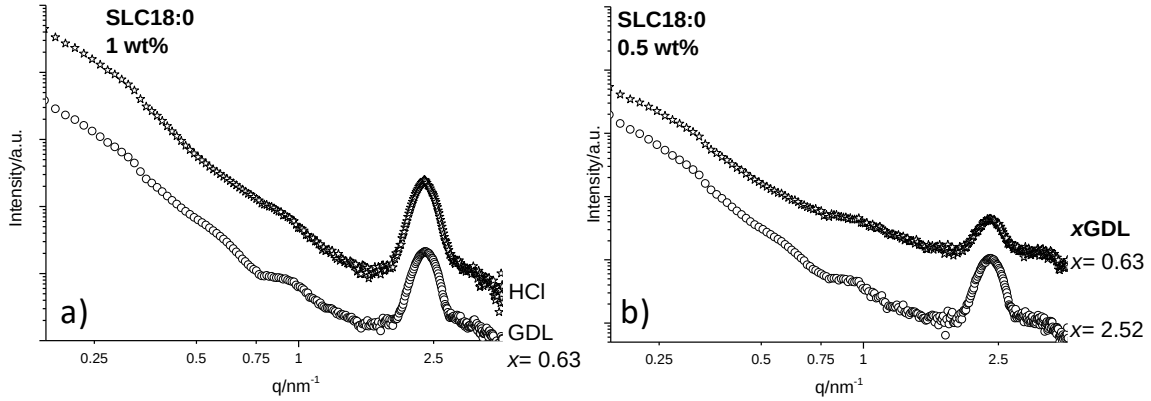

Figure S 3 – SAXS patterns of a) SLC18:0 1 wt% solution acidified with HCl (manually) and GDL (*x*= 0.63) and b) SLC18:0 0.5 wt% solution acidified with GDL at two different SLC18:0:*x*GDL molar ratios. The initial pH is 11 for all samples.

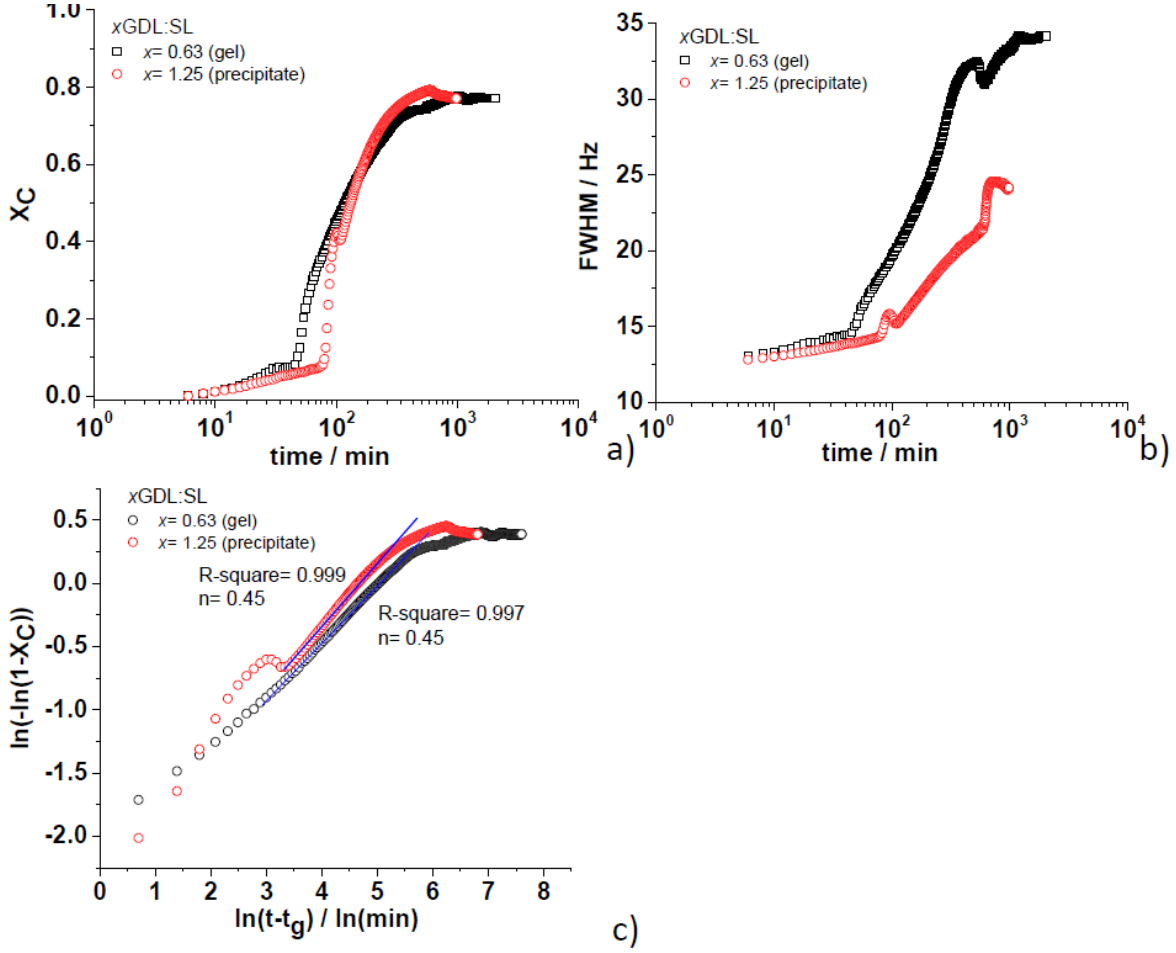

Figure S 4 – a) Time evolution of the molar fraction of SLC18:0 (Initial concentration is 2.5 wt% and pH 11) in the crystalline (fiber) phase upon addition of *x*GDL, *x* being the SLC18:0: *xGDL* molar ratio; X_C from the solution ^{1}H NMR spectra, as explained in the materials and method section. b) Time evolution of the full width at half maximum (FWHM); c) Avrami plot performed on X_C data in a).

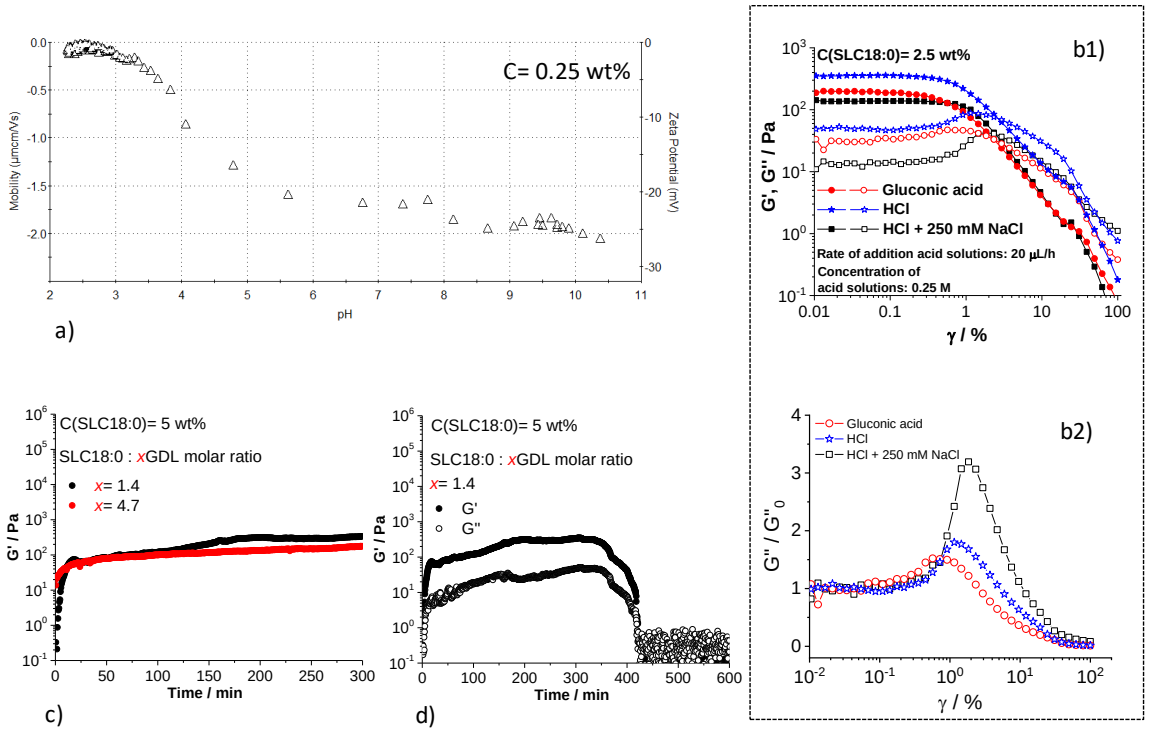

Figure S 5 – a) Overall electrophoretic mobility and ζ-potential evolution measured as a function of pH from pH ~11 to pH ~2 on a SLC18:0 solution at C= 0.25 wt% measured at 25 °C using a Malvern Zetasizer Nano ZS90 (Malvern Instruments). b1) Strain dependent storage (G') and loss (G'') moduli at a constant frequency (f = 1 Hz) for a SLC18:0 solution (V= 1 mL) prepared at C= 2.5 wt% and initial pH ~10. The acid solutions are composed of either HCl or gluconic acid, both at 0.25 M. Rate of addition is 20 µL/h. The gluconic acid solution is prepared from a 2 M GDL solution left at rest overnight and with final pH of 1.5, whereas GDL spontaneously hydrolyzes into gluconic acid in water. The experiments referred to with filled and empty squares are recorded on a solution containing additional 250 mM NaCl and of which the acidification has been performed with HCl (0.25 M). b2) Normalized loss (G''/G''_0) moduli shown in b1) by their respective values in the LVER as function of the shear strain γ. c-d) Time-resolved evolution of storage (G') and loss (G'') moduli measured at (f= 1 Hz, γ = 0.1%) on a SLC18:0 solution at C= 5 wt% and set at pH ~10. Acidification is performed with an excess of GDL, of which the molar ratio with respect to SLC18:0 are given in the figure.

References

(1) Ozbas, B.; Kretsinger, J.; Rajagopal, K.; Schneider, J. P.; Pochan, D. J. Salt-Triggered Peptide Folding and Consequent Self-Assembly into Hydrogels with Tunable Modulus. *Macromolecules* **2004**, *37*, 7331–7337.

(2) Franceschini, A.; Filippidi, E.; Guazzelli, E.; Pine, D. J. Dynamics of Non-Brownian Fiber Suspensions under Periodic Shear. *Soft Matter* **2014**, *10*, 6722–6731.

(3) Breedveld, V.; Nowak, A. P.; Sato, J.; Deming, T. J.; Pine, D. Rheology of Block Copolypeptide Solutions: Hydrogels with Tunable Properties. *Macromolecules* **2004**, *37*,

3943–3953.

(4) MacKintosh, F. C.; Käs, J.; Janmey, P. A. Elasticity of Semiflexible Biopolymer Networks. *Phys. Rev. Lett.* **1995**, *75*, 4425–4428.

(5) Hyun, K.; Wilhelm, M.; Klein, C. O.; Cho, K. S.; Nam, J. G.; Ahn, K. H.; Lee, S. J.; Ewoldt, R. H.; McKinley, G. H. A Review of Nonlinear Oscillatory Shear Tests: Analysis and Application of Large Amplitude Oscillatory Shear (LAOS). *Prog. Polym. Sci.* **2011**, *36*, 1697–1753.

(6) Mason, T. G.; Bibette, J.; Weitz, D. A. Elasticity of Compressed Emulsions. *Phys. Rev. Lett.* **1995**, *75*, 2051.

(7) Cloitre, M.; Borrega, R.; Leibler, L. Rheological Aging and Rejuvenation in Microgel Pastes. *Phys. Rev. Lett.* **2000**, *85*, 4819.

(8) Hyun, K.; Kim, S. H.; Ahn, K. H.; Lee, S. J. Large Amplitude Oscillatory Shear as a Way to Classify the Complex Fluids. *J. Nonnewton. Fluid Mech.* **2002**, *107*, 51–65.

(9) Pellens, L.; Gamez Corrales, R.; Mewis, J. General Nonlinear Rheological Behavior of Associative Polymers. *J. Rheol. (N. Y. N. Y).* **2004**, *48*, 379.

(10) O'Leary, L. E. R.; Fallas, J. A.; Bakota, E. L.; Kang, M. K.; Hartgerink, J. D. Multi-Hierarchical Self-Assembly of a Collagen Mimetic Peptide from Triple Helix to Nanofibre and Hydrogel. *Nat. Chem.* **2011**, *3*, 821–828.

(11) Tirtaatmadja, V.; Ta, K. C.; Jenkins, R. D. Rheological Properties of Model Alkali-Soluble Associative (HASE) Polymers: Effect of Varying Hydrophobe Chain Length. *Macromolecules* **1997**, *30*, 3271–3282.

(12) Raghavan, S. R.; Khan, S. A. Shear-induced Microstructural Changes in Flocculated Suspensions of Fumed Silica. *J. Rheol. (N. Y. N. Y).* **1995**, *39*, 1311.

(13) Parthasarathy, M.; Klingenberg, D. J. Large Amplitude Oscillatory Shear of ER Suspensions. *J. Nonnewton. Fluid Mech.* **1999**, *81*, 83–104.